Current Viewpoints on Oxide Adherence Mechanisms

J.L. Smialek
Lewis Research Center
Cleveland, Ohio

and

R. Browning
Ames Research Center
Moffett Field, California

NASA

NASA Technical Memorandum 87168

Current Viewpoints on Oxide Adherence Mechanisms

J.L. Smialek
Lewis Research Center
Cleveland, Ohio

and

R. Browning
Ames Research Center
Moffett Field, California

Prepared for the
One hundred and sixty-eighth Meeting of the Electrochemical Society
Las Vegas, Nevada, October 15–18, 1985

NASA

CURRENT VIEWPOINTS ON OXIDE ADHERENCE MECHANISMS

J.L. Smialek and R. Browning*
National Aeronautics and Space Administration
Lewis Research Center
Cleveland, Ohio 44135

SUMMARY

Additional hot stage Auger experiments have provided surface segregation data for NiCrAl ± Y or Zr alloys in agreement with other investigations. This data, combined with experimental and theoretical evidence of the Al_2O_3-metal bond strength, is presented in support of a chemical mechanism of Al_2O_3 scale adhesion. Both the detrimental effects of sulfur segregation and the beneficial effects of dopant segregation may be important. Chemical features of the dopants are compared in light of these proposed mechanisms, namely ΔH_f (sulfide), ΔH_f (oxide), electron orbital configuration, and insolubility in Ni.

INTRODUCTION

The rare-earth or oxygen-active dopant effect on oxide scale-metal adhesion has been dealt with in a large number of high temperature oxidation studies. These studies have produced a handful of elegant theories which are consistent with the many kinetic, morphological, and adhesive behavior of thermally grown scales. However, agreement is lacking as to which mechanism is the most fundamental to adhesion mainly because exceptions have been found for each proposal.

Recently some new postures have been taken on the question of Al_2O_3-MCrAl adhesion primarily as the result of hot stage Auger spectroscopy (refs. 1 to 3). These studies found substantial sulfur segregation only in undoped alloys and suggested that sulfur will serve to weaken the Al_2O_3-MCrAl bond and that the role of the Y dopant was to getter and bind sulfur in the bulk alloy in the form of Y-sulfides. Indeed, doping the alloy with Y_2S_3 instead of elemental Y rendered the dopant ineffective and allowed severe spallation to occur during cyclic oxidation (refs. 1 and 2). However, co-doping with both Y_2S_3 and additional Y in its elemental form restored the adherent characteristics of the scale. This evidence of the detrimental effect of sulfur segregation on the Al_2O_3-MCrAl bond and its prevention by Y doping appears irrefutable.

There is, however, an additional possible effect of the oxygen-active dopants, namely, bond enhancement — for these dopant elements also surface segregate and are likely to play an important role in the nature of the chemical bond at the exact oxide-metal interface. The first observation of Y-segregation was made by Bullock et al. in 1973 using an Auger and sputter profiling technique on an oxidized NiCrAlY alloy (ref. 4). Similarly, Auger and ball cratering revealed a Zr-rich interlayer on an oxidized NiCrAl + Zr alloy (ref. 5). Zr segregation at the surface of the same alloy has also been

---

*NASA Ames Research Center, Moffett Field, California 94035.

observed by hot stage Auger work (ref. 6), as have Y enrichments in other MCrAl alloys (ref. 3).

The purpose of this paper is to present our own hot stage Auger studies of surface segregation for an undoped NiCrAl and for Y or Zr-doped NiCrAl alloys. Special attention will also be given to past and recent surface science studies which suggest that oxygen-active dopants may also serve to increase the strength of the Al_2O_3-MCrAl bond.

EXPERIMENTAL PROCEDURE

The three NiCrAl alloys used in this study were multiphase $\gamma/\gamma'/\beta$ button castings used and characterized in a number of previous studies (refs. 5 to 8). The base alloy composition, Y (or Zr) dopant level, and amount of impurities is shown in table I. Cyclic oxidation was performed at 800 and 1100 °C in air on samples polished to a 600 grit finish. Hot stage Auger and XPS studies were performed at a base pressure of 5×10^{-10} torr after precleaning by Argon ion bombardment. Spectra were produced every 100 °C (from 450 to 750 °C) after 5 min anneals at each step. Auger/XPS analyses were also performed after partial in-situ oxidation at 10^{-6} torr O_2 for 5 min at temperature in order to study surface segregation in the presence of a thin oxide film. Also, the undoped NiCrAl alloy was studied after sputter coating with approximately 2 and 20 monolayers of Zr to elucidate the mechanism by which Zr prevents sulfur segregation. Details of the equipment, procedure, and spectra interpretation will be found in a more comprehensive study (ref. 9).

RESULTS

The results of the hot stage experiments are shown in figures 1 to 3. They basically confirm the results of earlier works which showed that sulfur segregates readily in undoped MCrAl's and is suppressed by the addition of oxygen-active dopants - in this case Y or Zr. It is important to note that this degree of sulfur segregation occurred even with only 10 ppm or less in the base alloy. Zr-doping prevented any observation of sulfur segregation by Auger techniques and very small S peaks were observed by XPS, but only up to 500 °C. Zr was observed to segregate instead quite heavily. A similar effect of Y-doping was observed, although small S peaks were observed in both Auger and XPS. Examples of the Auger spectra for the three alloys after heating to 750 °C are shown in figure 4. The substitution of the strong S peaks for the undoped alloy by Zr or Y peaks for the doped alloys is clearly evident.

The results of the 10^{-6} torr partial oxidation are also shown in figures 1 to 3. The basic changes here are an increase in the Al and O levels (from a previously decreasing level at 10^{-10} torr) and considerable peaks for Zr and Y. XPS, sensitive to depths appproximately three times those detected in Auger, found a continuous increase in both Zr or Y after each successive oxidation treatment. Thus, oxygen-active elements also segregate and suppress sulfur segregation at an aluminum oxide - NiCrAl interface.

The Auger spectra obtained after depositing two monolayers of Zr on the undoped NiCrAl (spectrum a) are shown in figure 5. Zr peaks were found to decrease on heating from 450 to 750 °C (spectra b to e), while sulfur again strongly segregated to the surface of the Zr film. This indicated that Zr

does not prevent S segregation by a simple site competition mechanism. Argon ion cleaning and repeating the experiment with 10 to 20 monolayers of Zr again failed to suppress sulfur segregation. This is approximately ten times the amount of Zr needed to tie up all the sulfur as ZrS_2 in the NiCrAl specimen containing 10 ppmm S. Thus, the mechanism of sulfur gettering in the Zr-doped bulk NiCrAl alloy may not be just by the formation of simple sulfides (ref. 2).

Cyclic oxidation data (1 hr cycles) of the three alloys at 800 and 1100 °C is shown in figure 6. As expected, the undoped NiCrAl spalled profusely and lost over 13 mg/cm² after 500 hr. By comparison the Zr-doped alloy gained 3 mg/cm² and the Y-doped alloy lost 1 mg/cm (it was not determined whether this weight loss occurred by spalling at the oxide-metal interface). Cycling at 800 °C, in the regime where the Auger studies were performed, produced minimal weight gain (approximately 0.1 mg/cm²) and no differentiation of alloys.

DISCUSSION

A. Sulfur Segregation (indirect effect)

It is suggested from the present results and previous studies that a major effect of the dopants is simply to prevent or retard sulfur segregation to the oxide-metal interface. Thus, the dopants act to <u>indirectly</u> improve scale adhesion by preventing bond weakening.

The detrimental effect of sulfur on oxide-metal bonding was first briefly suggested in a study of sulfur segregation and grain boundary embrittlement of Ni-base superalloys (ref. 10). The effectiveness of Y in preventing sulfur segregation and restoring scale adhesion was experimentally proven in the works of Smeggil, et al. (refs. 1 and 2). The bond weakening effect of sulfur at grain boundaries in metals has been modeled by quantum chemical molecular orbital techniques (ref. 11). This study found that sulfur (and other common impurities) served to pull electrons away from metal atoms by the formation of heteropolar M-S bonds and prevent these electrons from contributing to the stronger metallic-type bonds across the grain boundary. An analogous bond weakening argument is expected to apply to the Al_2O_3-S-NiCrAl system as well, although such a system has not as yet been modeled.

In addition to numerous reports of sulfur grain boundary segregation and embrittlement of superalloys, it was also found to promote creep cavitation because of its low surface energy (ref. 12). A comparable process could be envisioned to explain the unusual type of Kirkendall porosity formed at the oxide-metal interface. Substituting Zr (γ_S = 2.79 J/m²) or Y (γ_S = 1.16 J/m²) for S (γ_S = 0.078 J/m²) could prevent a surface energy driven cavitation at the interface due to growth stress in the oxide.

The gettering effect of the oxygen-active elements is undoubtedly related to the low free energies of formation of Y, Zr, or Hf-sulfides, and these values will be discussed in more detail later. Sulfur segregation appears to be prevented by dopant-sulfur interaction in the bulk alloy as opposed to direct site competition at the surface. This is indicated by the ineffectiveness of the Zr layer to prevent S segregation as well as the observation that S grain boundary segregation can be prevented by Zr additions to Ni alloys without any Zr grain boundary segregation (refs. 12 and 13). This mechanism of gettering was proposed by Smeggil et al. and was supported by their results.

3

One final comment on sulfur segregation to oxide-metal interfaces is appropriate. This deals with the effectiveness of dispersed oxides in serving as sulfur-sinks, also suggested by Smeggil (ref. 2). For Al_2O_3 particles, no auxiliary mechanism can be operative as would be the case for ThO_2 or Y_2O_3 particles, whose elemental cations also give rise to the adherence effect. Yet Al_2O_3 particles have been found to be effective for scale adhesion (ref. 14). It can be shown that 2 vol % of 100A particles can accommodate the extremely large value of >0.5 vol % of impurity and thus prevent segregation to the scale-metal interface (ref. 9).

B. Dopant Segregation (direct effect)

The above discussion has reviewed the detrimental effect of sulfur segregation and the role of oxygen-active dopants in preventing sulfur segregation. However, an additional effect of scale-metal <u>bond strengthening</u> may occur, for the dopants are also found to segregate at the interface.

The oxygen-active elements that cause adhesion are so called because of their negative values of ΔG_f of their oxides. Oxide-metal bonding properties have been found to correlate with ΔG_f (oxide). It is therefore suggested that this property may also benefit scale-metal adhesion when monolayers of these dopants are present at the interface. For example, liquid metal droplet contact angles on Al_2O_3 substrates have been analyzed to produce values for the work of adhesion (W_{AD}). These values were found to be linear functions of ΔG_f (metal oxide), as in figure 7 (ref. 15). A similar correlation was found for the friction coefficient of metal-sapphire sliding contacts in high vacuum, figure 8 (ref. 16). Also apparent are the deleterious effects of a chlorine exposure and the beneficial effects of an oxygen exposure (200 to 1000 Langmuirs). The Al_2O_3-metal bond has also been modeled using quantum chemical cluster calculations for the same metals used in the friction experiments (ref. 17). A qualitative correlation was found with the degree of anti-bonding orbital occupation for AlO_6 clusters and metals with small $-\Delta G_f$ (oxide), e.g., Ni, Cu, Ag, figure 9. The least occupation of these bond-weakening anti-bonding orbitals was obtained with Fe, which has the largest $-\Delta G_f$ (oxide). It was also pointed out that unoccupied metal-d orbitals favor selective occupation of only the bonding orbitals of the M(d)-O(2p) hybrids.

Another molecular orbital quantum chemical study has modeled the bonding of Y, Al, Ni atoms to Ni_9 clusters, and AlO_6, YO_6 clusters to Ni_9M, Al_{10} and Y_{10} clusters (ref. 18). The energy band structure for an AlO_6-Ni_{10} model is shown in figure 10. The metal 3d orbitals were found to hybridize with oxygen 2p orbitals as in the previous study. Similarly, the unoccupied metal d-orbitals served to stabilize oxygen 2p electrons. The actual binding energies for the clusters are shown in table II. These indicate that Y atoms are strongly bound to Ni_9 clusters and that AlO_6 clusters are more strongly bound to Y_{10} clusters than to Ni_{10} or Al_{10}. Thus, this theoretical study predicts a substantial bond enhancement should a few monolayers of Y exist between the Al_2O_3 scales and the nickel substrate, as was indicated by the Auger studies. It is expected that other chemically similar oxygen-active elements such as Zr will produce similar quantum chemical results, and the extent of this chemical similarity of many dopants will be discussed below. Other binding energies in table II indicate that yttrium oxide is not strongly bound to nickel nor is aluminum oxide strongly bound to dilute nickel-aluminum or nickel-yttrium alloys. These

4

results indicate that a discrete layer of Y_2O_3 does not strengthen the interface, nor is aluminum oxide strongly bound to pure nickel or nickel alloys.

C. Beneficial Attributes of Effective Dopants Elements

From the discussions above it appears that effective dopants: (1) are sulfur-active, (2) are oxygen-active, (3) possess unoccupied d-orbitals, and (4) surface segregate in Ni. The first property is clearly a requirement for elements to getter sulfur and prevent interfacial segregation of sulfur. The standard enthalpy of formation, $\Delta H°_{298}$ (M_xS_y) of a wide range of metal sulfides (approximately 40) is shown in figure 11. The stoichiometry of the sulfides is identical to that of the oxides with exceptions of WS_2, TaS_2, NbS_2 and V_2S_3. ΔG_f (M_xS_y) would be a more appropriate term to describe sulfide stability, however these were not available for nearly as many metals (ref. 19). For about ten metal sulfides, it was found that the free energy term was linearly related to the enthalpy by:

$$\Delta G_{1400\ K}\ (M_xS_y) = 0.90\ \Delta H°_{298}\ (M_xS_y) - 14\ kcal/mol\ S_2$$

with only approximately 10 kcal/mol error for any given sulfide. ΔH is therefore used as a relative indicator of sulfide stability. It can be readily seen from figure 11 that the most sulfur-active metals are those which are also effective dopants for oxide adhesion (filled circles for Sc, Y, Zr, La, Hf, Ce, Zr, Th).

The relative oxide stability, $\Delta H°_{298}$ (M_xO_y), is also shown in figure 11. Again the oxygen-active elements are those responsible for adhesion (filled circles), as was recognized in many prior works on scale adhesion. (Again, the free energy was found to be a linear function of enthalpy for approximately 25 metals (ref. 20):

$$\Delta G_{1400\ K}\ (M_xO_y) = 0.92\ \Delta H°_{298}\ (M_xO_y) - 46\ kcal/mol\ O_2,$$

and $\Delta H°$ was used as a relative index of oxide stability. The critical point of this figure is that all the most oxygen-active elements are also the most sulfur-active. Thus, no one element could be used to illustrate the indirect dopant effect (S gettering) without also having the potential of the direct effect (Al_2O_3-NiCrAl bond strengthening), and vice versa. Thus, the separation of the relative contributions of these phenomena becomes a problem.

There is some direct correlation of sulfide and oxide enthalpies given by:

$$\Delta H°_{298}\ (M_xS_y)\ 0.56\pm0.22\ \Delta H°_{298}\ (M_xO_y)$$

The regularity of the sulfide/oxide stability factor is shown more clearly by following the metals by atomic number row by row in the periodic table. In fact, rows 4, 5, and 6 nearly superimpose on these curves and give a very regular change in ΔH(Sulfide)/ΔH (Oxide) as shown in figure 12. It is interesting to point out that on a kcal/gm atom metal basis (fig. 11) a distinct drop in sulfide stability is observed between Sc and Ti, Zr and Nb, and Hf and Ta, which corresponds to a boundary between effective and noneffective alloy elements with respect to adhesion. It is also important to point out that on a per mol S_2 or O_2 basis, both group I (Na, K) and group II (Mg, Ca, Sr, Ba) elements also rank as highly sulfur active, while group II ranks

5

as highly oxygen-active as well However, the effectiveness of these elements as adherence additives is questionable and has never been reported.

In order for the dopants to be effective as bond strengtheners (direct effect) they must segregate to the oxide-metal interface. The relative enrichment of a solute at a surface has been formulated as a function of exp $(-\Delta H(segr.)/RT)$ where $\Delta H(segr.) = \Delta E(surf.) - \Delta E(strain) - \Delta H(mix.)$ (ref. 21). $\Delta E(surf)$ is the change in surface energy after segregation, $\Delta E(strain)$ is the strain energy increase realized by insertion of alloy elements of different atomic size, and $\Delta H(mix.)$ is the enthalpy of dissolution incurred by alloying. Thus, low surface energy, high strain energy, and endothermic or low solubility alloying elements will tend to segregate the greatest. It has been pointed out that Y and Zr have very high surface energies, therefore, this factor will lessen segregation. However, they do have very large atomic radii (2.27 and 2.16 versus 1.62 A) and are nearly insoluble in Ni, and these factors favor a lowering of the overall system energy by segregating out of the lattice to a free surface or interface. Sulfur is also very insoluble in nickel from elec-tronegativity considerations, has a low surface energy, and is also predictably a strong segregant.

A summary of all the factors discussed in this paper as important to a chemical bond mechanism of adherence is shown in figure 13 for the salient portion of the periodic table. The dopants giving rise to Al_2O_3-MCrAl adhesion (in bold outline) are seen to have only partial occupation of the d-orbitals in concert with the molecular orbital cluster models. High $-\Delta H_f$ (oxide) values are evident in concert with the work of adhesion, contact shear strength, and molecular orbital predictions on Al_2O_3 - metal bond strengths. Low solubilities exist for these dopants, which is not the case for the elements immediately to the right (Ti, Nb, Ta), which are not effective dopants: And finally, high $-\Delta H_f$ (sulfide) values exist for this group which is a prere-quisite for effective sulfur gettering.

CONCLUDING REMARKS

This paper has presented Auger work reinforcing the findings of Smeggil and co-workers that sulfur segregation prevents Al_2O_3 scale - NiCrAl adher-ence and doping with sulfur-active elements prevents sulfur segregation, resulting in strong scale adhesion. However, we have also presented arguments suggesting that the interfacial bond may actually be _strengthened_ by the segre-gation of the _dopants_ themselves. These arguments are based on a number of experimental and theoretical studies which have found stronger bonding between Al_2O_3 and metals with a high chemical affinity for oxygen. While the deleter-ious effects of sulfur segregation had been conclusively proven, the deter-mination of the relative degree of bond strengthening due to the dopants is likely to be a much more difficult task. This is because all the oxygen-active elements are also sulfur-active. The spalling behavior of impurity-free MCrAl alloys or molecular orbital studies of the Al_2O_3-S-Ni interface may provide the next level of understanding to this continuing and fascinating puzzle.

REFERENCES

1. A.W. Funkenbusch, J.G. Smeggil, N.S. Bornstein, _Metall. Trans. A_, _16A_, 1164 (1985).

2. J.G. Smeggil, A.W. Funkenbusch, N.S. Bornstein, <u>Metall. Trans.</u>, Accepted for Publication.

3. K.L. Luthra, C.L. Briant, Electrochemical Society 1985 Spring Meeting, Cincinnati, OH; Extended Abstracts, 26 (1985).

4. E. Bullock, C. Lea, M. McLean, <u>Met. Sci.</u>, <u>13</u>, 373 (1979).

5. L.A. Larson, M. Prutton, H. Poppa, J. Smialek, <u>J. Vac. Sci. Technol.</u>, <u>20</u>, 1403 (1982).

6. M.M. El Gomati, C. Walker, D.C. Peacock, M. Prutton, <u>Corros. Sci.</u>, <u>25</u>, 351 (1984).

7. M.M. El Gomati, C.G.H. Walker, D.C. Peacock, M. Prutton, H.E. Bishop, R.M.H. Hawes, J.L. Smialek, <u>Surf. Sci.</u>, <u>152/153</u>, 917 (1984).

8. J.L. Smialek, R. Gibala, <u>Metall. Trans. A</u>, <u>14A</u>, 2143 (1983).

9. I) R. Browning, C. Park, F.A. Marks, J. Smialek, II) R. Browning, C. Park, F.A. Marks, C. Papageorgopoulas; III) J. Smialek, R. Browning, to be Published.

10. C.L. Briant, R.A. Mulford, <u>Metall. Trans. A</u>, <u>13A</u>, 745 (1982).

11. R.P. Messmer, C.L. Briant, <u>Acta Metall.</u>, <u>30</u>, 457 (1982).

12. C.L. White, J.H. Schniebel, R.A. Padgett, <u>Metall. Trans. A</u>, <u>14A</u>, 595 (1983).

13. W.C. Johnson, J.E. Doherty, B.H. Kear, A.F. Giamel, <u>Scr. Metall.</u>, <u>8</u>, 971 (1974).

14. J.K. Tien, F.S. Pettit, <u>Metall. Trans.</u>, <u>3</u>, 1587 (1972).

15. J.E. McDonald, J.G. Eberhart, <u>Trans. Aime</u>, <u>233</u>, 512 (1965).

16. S.V. Pepper, <u>J. Appl. Phys.</u>, <u>47</u>, 801 (1976).

17. K.H. Johnson, S.V. Pepper, <u>J. Appl. Phys.</u>, <u>53</u>, 6634 (1982).

18. A.B. Anderson, S.P. Mehendru, J.L. Smialek, J. <u>Electrochem. Soc.</u>, <u>132</u>, 1695 (1985).

19. K.C. Mills, Thermodynamic Data for Inorganic Sulfides, Selenides and Tellurides, Butterworth, London (1974).

20. I. Brian, O. Knacke, O. Kubaschewski, Thermochemical Properties of Inorganic Substances, Springer-Verlag, New York (1973), Supplement (1977).

21. G.A. Somorjai, Chemistry in Two Dimensions: Surfaces, Cornell University Press, Ithaca (1981).

TABLE I. - CHEMICAL COMPOSITION OF NiCrAl ALLOYS

Wt %				Weight, ppm				
Ni	Cr	Al	Y(OR Zr)	S	P	Sn	V	Zn
BAL	15	13	0, 0.5	<10	100	410	60	70

TABLE II. - YTTRIUM-ENHANCED MOLECULAR ORBITAL BINDING ENERGIES FOR Al_2O_3-Ni (ANDERSON, et al., 1985)

Surface species		Substrate cluster	Binding energy, eV
Ni	on	Ni_9	3.4
Al	on	Ni_9	6.3
Y	on	Ni_9	10.4
AlO_6^{6-}	on	Ni_{10}	4.0
YO_6^{6-}	on	Ni_{10}	3.9
AlO_6^{6-}	on	$AlNi_9$	4.0
AlO_6^{6-}	on	YNi_9	5.8
AlO_6^{6-}	on	Al_{10}	4.8
AlO_6^{6-}	on	Y_{10}	12.8
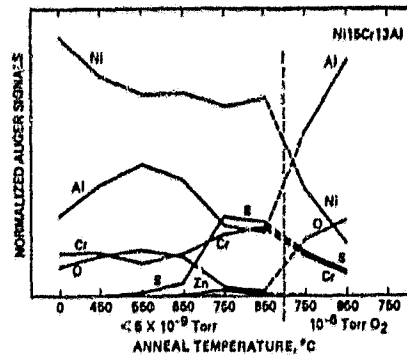
Figure 1. - Surface segregation in undoped
NICrAl.
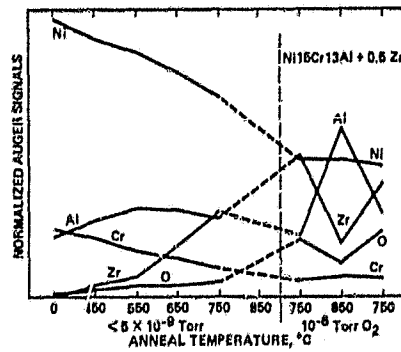
Figure 2. - Zr surface segregation in Zr-
doped NICrAl.
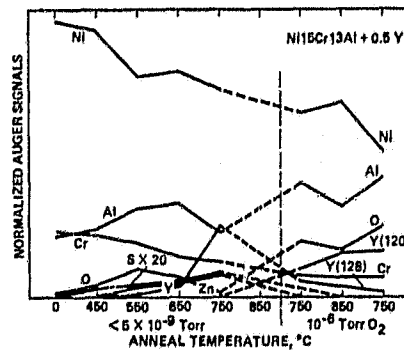
Figure 3. - Y surface segregation in Y-doped
NICrAl.
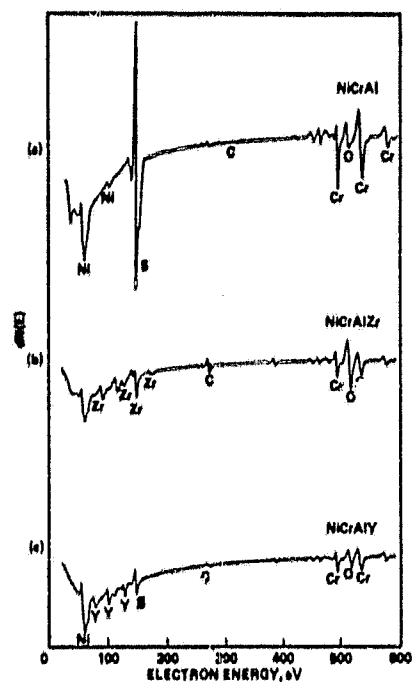
Figure 4. – dN(E) versus E Auger spectra after 750 °C vacuum annealing.
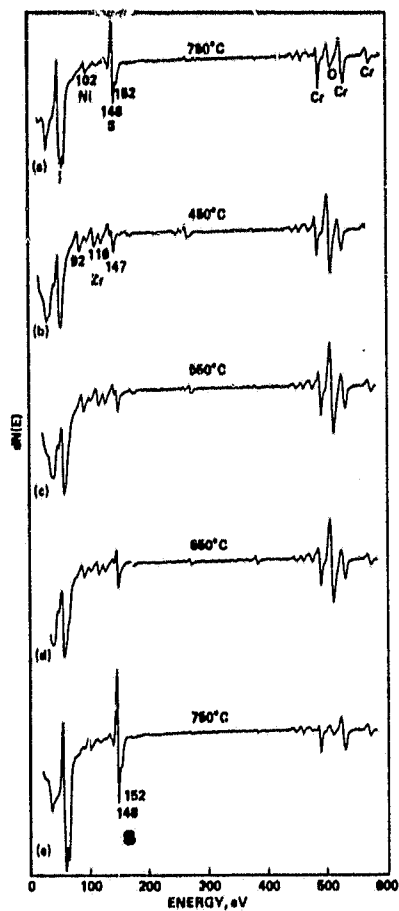
Figure 5. – Comparison of sulfur segregation in undoped NiCrAl before (a) and after (b to e) coating with 2 monolayers of Zr.
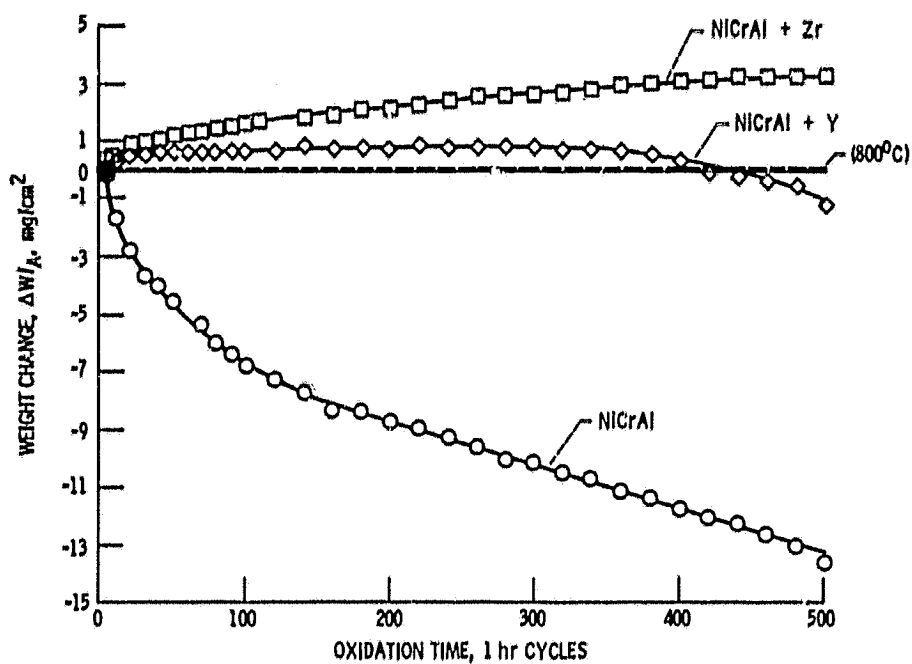
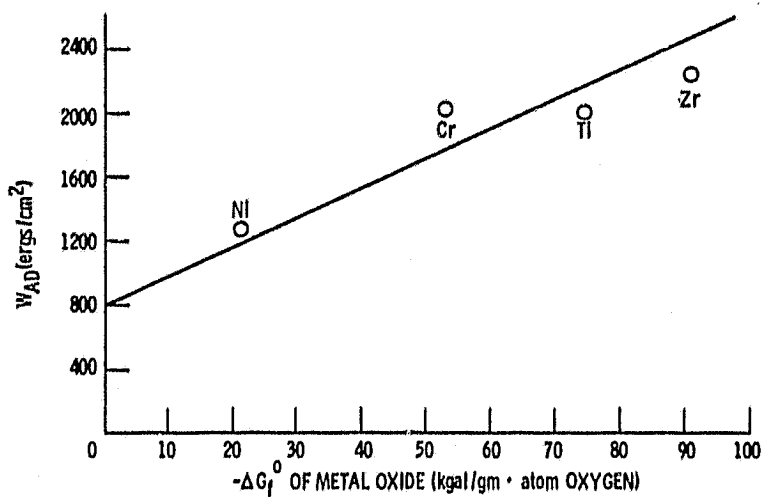Figure 6. - 800° and 1100 °C cyclic oxidation of undoped, Zr-doped, and Y-doped NiCrAl alloys.

Figure 7. - Correlation of work of adhesion for liquid metal-sapphire contacts and free energy of metal oxides (McDonald and Ebehart, 1965).
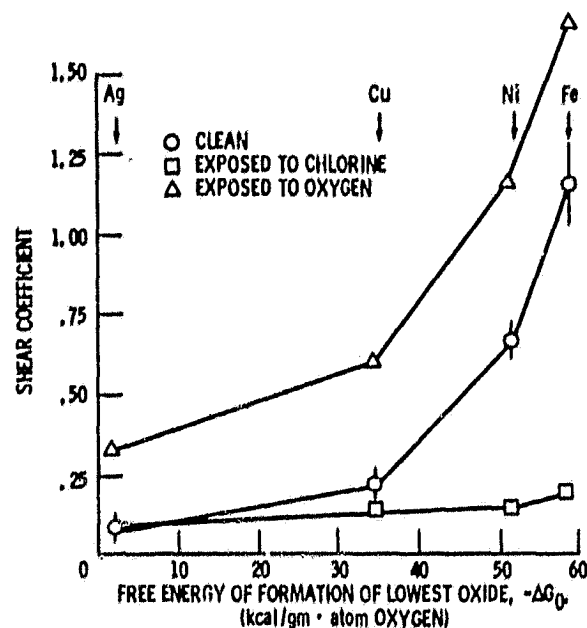
Figure 8. - Correlation of metal-sapphire contact strengths with ΔG_f^0 of metal oxides (Pepper, 1976).
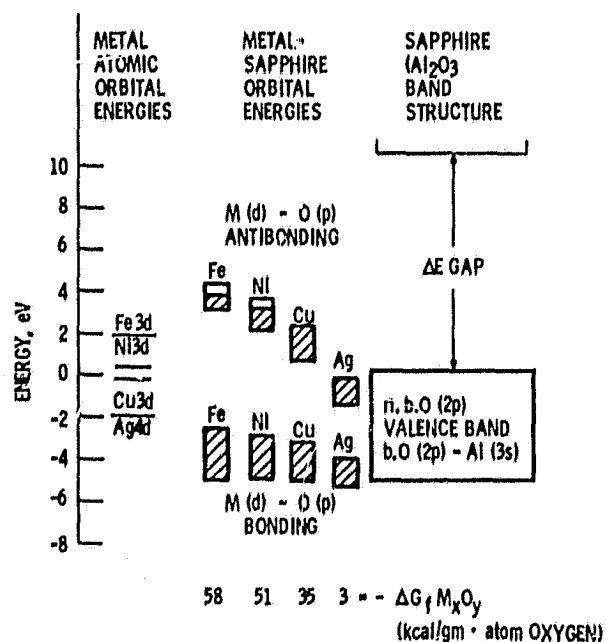

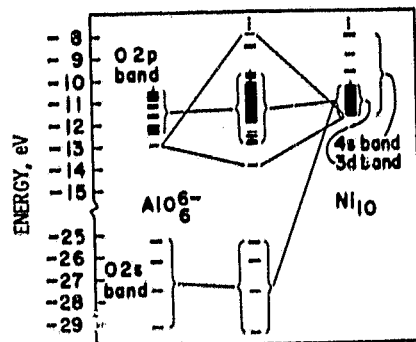Figure 9. - Molecular orbital energy levels for various metal-sapphire interfaces (Johnson and Pepper, 1982).

Figure 10. – Molecular orbital energy
levels showing bond stabilizations be-
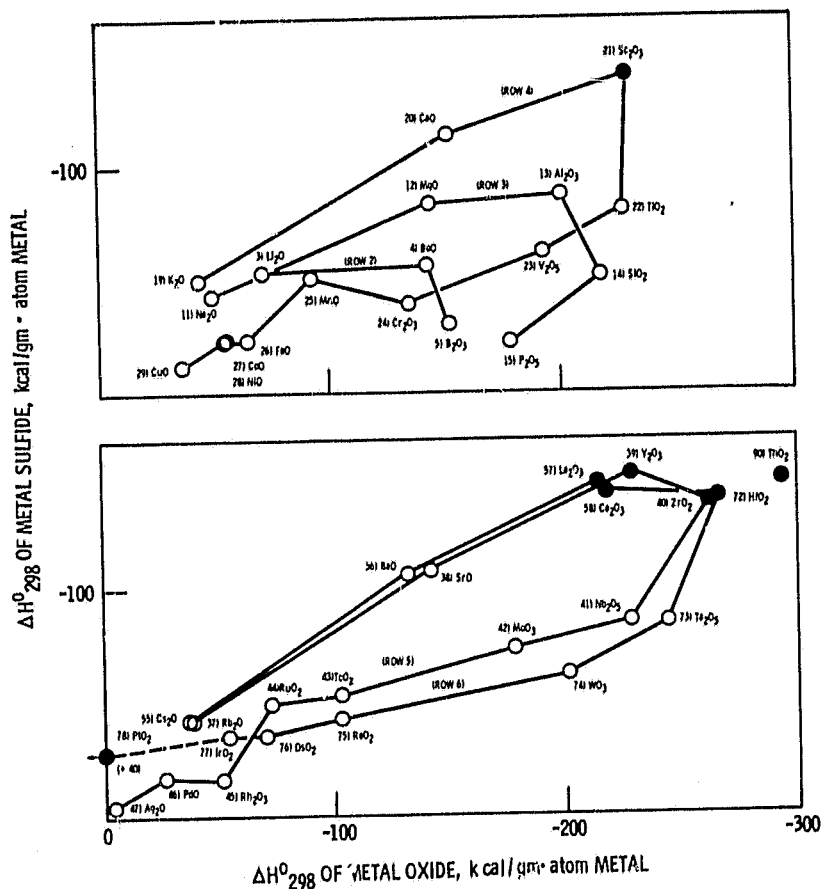tween AlO_6 and Ni_{10} clusters (Ander-
son, et. al., 1985).

Figure 11. – Correlation and periodicity of metal sulfide and metal oxide stabilities:
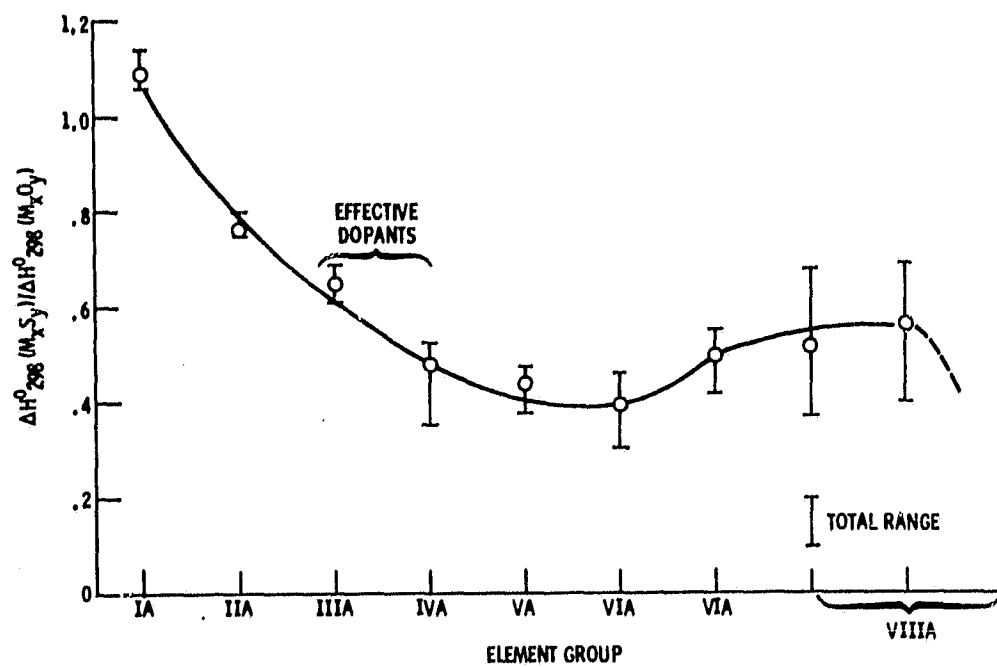$\Delta H^0_{298} (M_xS_y) \sim 0.56 \pm 0.22 \Delta H^0_{298} (M_xO_y)$.

Figure 12. - Periodic behavior of relative sulfide/oxide stabilities. (Average of Rows 4, 5, 6 in periodic table).

KEY:

ATOMIC NO.	METAL OXIDE
	• OUTER ELECTRONS
	• $-\Delta H^o_{f,298}$ METAL OXIDE
	• $-\Delta H^o_{f,298}$ METAL SULFIDE (kcal/mole O_2, S_2)
	• MAX. SOLUBILITY IN Ni (ATOMIC PERCENT)

II A	III A	IV A	V A	VI A	VII A	VIII A		III B	IV B	V B	VI B
12 MgO $3s^2$ 288 166 <0.24%	21 Sc_2O_3 $3d^14s^2$ 304 186 ---	22 TiO_2 $3d^24s^2$ 226 80 15%	23 V_2O_5 $3d^34s^2$ 149 84 43%	24 Cr_2O_3 $3d^54s^1$ 180 54 50%	25 MnO $3d^54s^2$ 184 102 100%	26 NiO $3d^84s^2$ 116 44 ---		13 Al_2O_3 $3s^2p^1$ 267 162 21%	14 SiO_2 $3s^2p^2$ 217 51 17.6%	15 P_2O_5 $3s^2p^3$ 143 18 0.32%	16 SO_2 $3s^2p^4$ <.011%
20 CaO $4s^2$ 304 228 ---	39 Y_2O_3 $4d^15s^2$ 303 200 0.14%	40 ZrO_2 $4d^25s^2$ 262 138 0.6%	41 Nb_2O_5 $4d^45s^1$ 182 85 13.5%								
38 SrO $5s^2$ 284 216 ---	57 La_2O_3 $5d^16s^2$ 286 194 0%	72 HfO_2 $5d^26s^2$ 266 140 0%	73 Ta_2O_5 $5d^36s^2$ 196 85 15.4%								
56 BaO $6s^2$ 264 212 0.08%											

| 58 Ce_2O_3 $4f^15d^16s^2$ 290 190 0% |
| 90 ThO_2 $6d^27s^2$ 293 150 <0.002% |

Figure 13. – Periodic elemental properties relevant to chemical bonding mechanisms.

1. Report No.	2. Government Accession No.	3. Recipient's Catalog No.
NASA TM-87168		

4. Title and Subtitle	5. Report Date
Current Viewpoints on Oxide Adherence Mechanisms	
	6. Performing Organization Code
	505-63-01

7. Author(s)	8. Performing Organization Report No.
J.L. Smialek and R. Browning	E-2806
	10. Work Unit No.

9. Performing Organization Name and Address	11. Contract or Grant No.
National Aeronautics and Space Administration Lewis Research Center Cleveland, Ohio 44135	
	13. Type of Report and Period Covered

12. Sponsoring Agency Name and Address	Technical Memorandum
National Aeronautics and Space Administration Washington, D.C. 20546	14. Sponsoring Agency Code

15. Supplementary Notes

16. Abstract

Additional hot stage Auger experiments have provided surface segregation data for NiCrAl $\pm$ Y or Zr alloys in agreement with other investigations. This data, combined with experimental and theoretical evidence of the Al_2O_3-metal bond strength, is presented in support of a chemical mechanism of Al_2O_3 scale adhesion. Both the detrimental effects of sulfur segregation and the beneficial effects of dopant segregation may be important. Chemical features of the dopants are compared in light of these proposed mechanisms, namely ΔH_f (sulfide), ΔH_f (oxide), electron orbital configuration, and insolubility in Ni.

17. Key Words (Suggested by Author(s))	18. Distribution Statement
Oxide adherence; Al_2O_3 scales; NiCrAl alloys; Oxidation	Unclassified – unlimited STAR Category 26

19. Security Classif. (of this report)	20. Security Classif. (of this page)	21. No. of pages	22. Price*
Unclassified	Unclassified		